[2] T. C. Edwards and R. P. Owens, "2–18 GHz dispersion measurements on 10–100 Ω microstrip lines on sapphire," *IEEE Trans. Microwave Theory Tech.*, vol. MTT-24, pp. 506–513, Aug. 1976.
[3] N. G. Alexopoulos and C. M. Krowne, "Characteristics of single and coupled microstrips on anisotropic substrates," *IEEE Trans. Microwave Theory Tech.*, vol. MTT-26, pp. 387–393, June 1978.
[4] N. G. Alexopoulos, "Integrated-circuit structures on anisotropic substrates," *IEEE Trans. Microwave Theory Tech.*, vol. MTT-33, pp. 847–881, Oct. 1985.
[5] M. Horno, "Quasistatic characteristics of microstrip on arbitrary anisotropic substrates," *Proc. IEEE*, vol. 67, pp. 1033–1034, Aug. 1980.
[6] S. K. Koul and B. Bhat, "Inverted microstrip and suspended microstrip with anisotropic substrates," *Proc. IEEE*, vol. 70, pp. 1230–1231, Oct. 1982.
[7] A-M. A. El-Sherbiny, "Hybrid mode analysis of microstrip lines on anisotropic substrates," *IEEE Trans. Microwave Theory Tech.*, vol. MTT-29, pp. 1261–1265, Dec. 1981.
[8] M. Kobayashi, "Frequency dependent characteristics of microstrips on anisotropic substrates," *IEEE Trans. Microwave Theory Tech.*, vol. MTT-30, pp. 2054–2057, Nov. 1982.
[9] H. Yang and N. G. Alexopoulos, "Uniaxial and biaxial substrate effects on finline characteristics," *IEEE Trans. Microwave Theory Tech.*, vol. MTT-35, pp. 24–29, Jan. 1987.
[10] C. M. Krowne, A. A. Mostafa, and K. A. Zaki, "Slot and microstrip guiding structures using magnetoplasmons for nonreciprocal millimeter-wave propagation," *IEEE Trans. Microwave Theory Tech.*, vol. 36, pp. 1850–1860, Dec. 1988.
[11] G. E. Mariki and C. Yeh, "Dynamic three-dimensional TLM analysis of microstriplines on anisotropic substrate," *IEEE Trans. Microwave Theory Tech.*, vol. MTT-33, pp. 789–799, Sept. 1985.
[12] J. L. Tsalamengas, N. K. Uzunoglu, and N. G. Alexopoulos, "Propagation characteristics of a microstrip line printed on a general anisotropic substrate," *IEEE Trans. Microwave Theory Tech.*, vol. MTT-33, pp. 941–945, Oct. 1985.
[13] T. Itoh and R. Mittra, "A technique for computing dispersion characteristics of shielded microstrip lines," *IEEE Trans. Microwave Theory Tech.*, vol. MTT-22, pp. 896–898, Oct. 1974.
[14] T. Itoh, "Analysis of microstrip resonators," *IEEE Trans. Microwave Theory Tech.*, vol. MTT-22, pp. 946–952, Nov. 1974.

Frequency-Dependent Characteristics of Shielded Broadside Coupled Microstrip Lines on Anisotropic Substrates

T. Q. Ho and B. Beker

Abstract—**In this paper, a spectral-domain technique is applied to compute the propagation characteristics of a shielded broadside coupled microstrip line printed on homogeneous uniaxial and biaxial substrates. The formulation derives the Green's functions for even and odd modes of the guiding structure via the transformed fourth-order differential equations. The analysis includes anisotropic substrates which are simultaneously characterized by both $[\epsilon]$ and $[\mu]$ tensors. This rigorous full-wave approach to the solution of the problem is shown to yield results agreeing well with the existing data. The propagation characteristics are studied with respect to different line width/thickness ratios as well as to the material substrate parameters.**

Manuscript received October 15, 1990; revised January 15, 1991.
The authors are with the Department of Electrical and Computer Engineering, University of South Carolina, Columbia, SC 29208.
IEEE Log Number 9144277.

I. Introduction

Among the various E-plane transmission line structures available for practical applications at microwave and millimeter-wave frequencies, the broadside coupled microstrip line is one of the most commonly used. In order to accurately design MIC circuits using this structure, the effect of dispersion should be carefully considered. One of the first studies of a broadside coupled microstrip line on isotropic substrates was carried out by Allen *et al.* [1]. Subsequently, Bornemann [2] also examined the dispersion characteristics of similar structures, however, without providing numerical results for the even-mode case. More recently, Mizuno *et al.* [3] have studied the same structure using a rigorous analysis to calculate dispersion properties of both the even and odd modes.

While isotropic media are frequently employed as substrates in circuits of this type, at higher frequency they may exhibit anisotropic properties as well. To account for such effects, D'Assunçaso *et al.* [5] have used the method of moments to study the broadside coupled line with no sidewalls on anisotropic substrates. However, this approach is quasi-static, so the results are limited to low frequencies. As an alternative, Koul *et al.* [6] presented a technique which is based on the transverse transmission line method for analyzing broadside coupled circuits of this kind using anisotropic media. Unfortunately, in all of the aforementioned works, the formulation of the problem considered materials characterized by tensor permittivity alone, and, in some cases, the analysis was further restricted to uniaxial substrates.

In this paper, the spectral-domain method is extended to study a shielded broadside coupled microstrip line along the E plane of the waveguide printed on anisotropic medium. The problem is generalized so that both dielectric and magnetic anisotropy effects are included in the formulation. The analysis is rigorously performed so that accurate full-wave solutions may be obtained. The two transformed fourth-order differential equations, which can be obtained from Maxwell's curl equations, yield solutions that lead to the derivation of the Green's functions for both the even- and the odd-mode case. The characteristic equation for the propagation constant is formed by applying the Galerkin method in the Fourier transform domain. Numerical results for the broadside coupled line are computed for a special isotropic case and are compared with the ones obtained in [3]. Good agreement for the effective dielectric constant is observed in the computed data throughout the selected w/b (strip-guide width) range. Additional examples exhibiting the behavior of the effective dielectric and propagation constants of the line on various anisotropic substrates including sapphire, boron nitride, filled PTFE (glass cloth), PTFE cloth, and lithium niobate are also presented.

II. Formulation

The broadside coupled microstrip line structure, shown in Fig. 1(a), consists of a thin substrate material layer characterized by both $[\epsilon]$ and $[\mu]$ biaxial tensors which is suspended inside a metal housing with dimensions a and b. The substrate, of thickness $2h_1$, is assumed to be lossless and is uniformly extended in the z direction. To simplify the analysis, the metal strips whose width is w are also assumed to be perfectly conducting and infinitely thin in the x direction. The medium properties of the substrate are characterized by diagonal biaxial

0018-9480/91/0600-1021$01.00 ©1991 IEEE

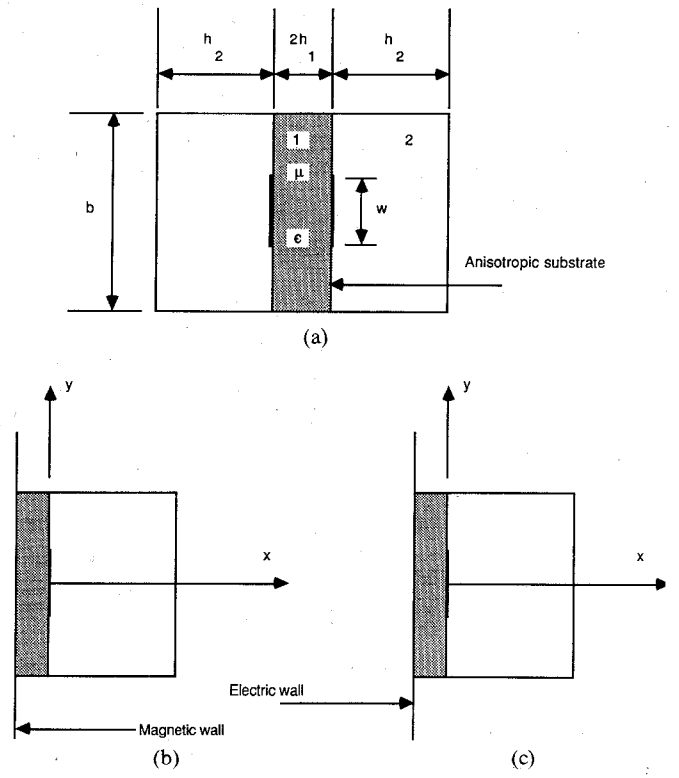

Fig. 1. (a) The geometry of a broadside coupled microstrip line. (b) Its equivalence for even mode. (c) Its equivalence for odd mode.

tensors of rank 2, that is, by

$$[\epsilon] = \epsilon_0 \begin{vmatrix} \epsilon_{xx} & 0 & 0 \\ 0 & \epsilon_{yy} & 0 \\ 0 & 0 & \epsilon_{zz} \end{vmatrix} \tag{1a}$$

$$[\mu] = \mu_0 \begin{vmatrix} \mu_{xx} & 0 & 0 \\ 0 & \mu_{yy} & 0 \\ 0 & 0 & \mu_{zz} \end{vmatrix} \tag{1b}$$

with ϵ_0 and μ_0 denoting the free-space permittivity and permeability, respectively.

The vector wave equations for the components of the electric and magnetic fields can readily be shown to have the following form:

$$\nabla \times \left([\mu]^{-1} \cdot \nabla \times \boldsymbol{E}\right) - k_0^2 [\epsilon] \cdot \boldsymbol{E} = 0 \tag{2a}$$

$$\nabla \times \left([\epsilon]^{-1} \cdot \nabla \times \boldsymbol{H}\right) - k_0^2 [\mu] \cdot \boldsymbol{H} = 0. \tag{2b}$$

When Fourier transforms of these equations, defined via an integral relation

$$\tilde{\Phi}(x,\alpha) = \int_{-b/2}^{b/2} \Phi(x,y) e^{j\alpha y}\, dy \tag{3}$$

where α is the discrete transform variable, are taken, they lead directly to the two differential equations having the form of [7]

$$\frac{d^4}{dx^4}\tilde{E}_{z,y} + f_1 \frac{d^2}{dx^2}\tilde{E}_{z,y} + f_2 \tilde{E}_{z,y} = 0. \tag{4}$$

In this geometry, the broadside coupled microstrip can support both even and odd modes. The even-mode case will be obtained when the magnetic wall is placed at $x = -h_1$ to cut the problem into two halves. Similarly, the electric wall can be put at the same location, thereby corresponding to the boundary conditions satisfied by the odd mode. These respective equivalent problems are shown in parts (b) and (c) of Fig. 1. The boundary conditions require that the tangential magnetic fields vanish at the magnetic wall for the even case and that the tangential electric fields be zero at the electric wall for the odd-mode case. By applying these conditions to the general solutions of equations (4) in the spectral domain, expressions for the fields in region 1 can be derived. For the even case, the fields are written as follows:

$$\tilde{H}_y^{\mathrm{I}}(x,\alpha) = -\left(j\omega\mu_0\mu_{yy}\right)^{-1}\left\{p_2 A_n^* \sin\gamma_1^a(x+h_1) + p_1 B_n^* \sin\gamma_1^b(x+h_1)\right\} \tag{5a}$$

$$\tilde{H}_z^{\mathrm{I}}(x,\alpha) = -\left(j\omega\mu_0\mu_{zz}\right)^{-1}\left\{p_4 A_n^* \sin\gamma_1^a(x+h_1) + p_3 B_n^* \sin\gamma_1^b(x+h_1)\right\} \tag{5b}$$

$$\tilde{E}_y^{\mathrm{I}}(x,\alpha) = p_6 A_n^* \cos\gamma_1^a(x+h_1) + p_5 B_n^* \cos\gamma_1^b(x+h_1) \tag{5c}$$

$$\tilde{E}_z^{\mathrm{I}}(x,\alpha) = A_n^* \cos\gamma_1^a(x+h_1) + B_n^* \cos\gamma_1^b(x+h_1) \tag{5d}$$

with constants p_1 to p_6 defined by

$$p_1 = \gamma_1^b + \beta\left(\alpha p_5 \epsilon_{yy}/\epsilon_{xx} + \beta\epsilon_{zz}/\epsilon_{xx}\right)/\gamma_1^b \tag{6a}$$

$$p_2 = \gamma_1^a + \beta\left(\alpha p_6 \epsilon_{yy}/\epsilon_{xx} + \beta\epsilon_{zz}/\epsilon_{xx}\right)/\gamma_1^a \tag{6b}$$

$$p_3 = -\alpha\left(\alpha p_5 \epsilon_{yy}/\epsilon_{xx} + \beta\epsilon_{zz}/\epsilon_{xx}\right)/\gamma_1^b - p_5\gamma_1^b \tag{6c}$$

$$p_4 = -\alpha\left(\alpha p_6 \epsilon_{yy}/\epsilon_{xx} + \beta\epsilon_{zz}/\epsilon_{xx}\right)/\gamma_1^a - p_6\gamma_1^a \tag{6d}$$

$$p_5 = \left(\left(\gamma_1^b\right)^2 - e_1\right)/e_2 \tag{6e}$$

and

$$p_6 = \left(\left(\gamma_1^a\right)^2 - e_1\right)/e_2. \tag{6f}$$

Here β is the propagation constant in the z direction; the parameters γ_1^a and γ_1^b are the propagation constants in the x direction within region 1; γ_2 is the constant for region 2; and k_0 denotes the propagation constant of free space. The field components for the odd-mode case can simply be obtained by interchanging terms appearing in (5) from $\sin\gamma_1^{a,b}(x+h_1)$ to $-\cos\gamma_1^{a,b}(x+h_1)$ and $\cos\gamma_1^{a,b}(x+h_1)$ to $\sin\gamma_1^{a,b}(x+h_1)$. The fields inside the isotropic region 2, $\tilde{H}_y^{\mathrm{II}}(x,\alpha)$, $\tilde{H}_z^{\mathrm{II}}(x,\alpha)$, $\tilde{E}_y^{\mathrm{II}}(x,\alpha)$, and $\tilde{E}_z^{\mathrm{II}}(x,\alpha)$ are given elsewhere [8] and therefore will not be repeated here.

In order to obtain the Green's function for the broadside coupled structure, the appropriate boundary conditions at $x = 0$ must be enforced:

$$\tilde{E}_y^{\mathrm{I}} = \tilde{E}_y^{\mathrm{II}} \tag{7a}$$

$$\tilde{E}_z^{\mathrm{I}} = \tilde{E}_z^{\mathrm{II}} \tag{7b}$$

$$\tilde{H}_y^{\mathrm{I}} - \tilde{H}_y^{\mathrm{II}} = \tilde{J}_z \tag{7c}$$

$$\tilde{H}_z^{\mathrm{I}} - \tilde{H}_z^{\mathrm{II}} = -\tilde{J}_y. \tag{7d}$$

After some mathematical manipulations, the Fourier transforms of the current densities on the conducting strips and the tangential fields in the region of the air–dielectric interface can be related to the impedance function by the following matrix expression:

$$\begin{bmatrix} \tilde{Z}_{zz}(\alpha,\beta) & \tilde{Z}_{zy}(\alpha,\beta) \\ \tilde{Z}_{yz}(\alpha,\beta) & \tilde{Z}_{yy}(\alpha,\beta) \end{bmatrix} \begin{bmatrix} \tilde{J}_z(\alpha) \\ \tilde{J}_y(\alpha) \end{bmatrix} = \begin{bmatrix} \tilde{E}_{zs}(\alpha) \\ \tilde{E}_{ys}(\alpha) \end{bmatrix} \tag{8}$$

wherein the individual elements are given by

$$\tilde{Z}_{zz}(\alpha,\beta) = \tilde{Y}_{yy}(\alpha,\beta)/\Delta \tag{9a}$$

$$\tilde{Z}_{zy}(\alpha,\beta) = -\tilde{Y}_{zy}(\alpha,\beta)/\Delta \tag{9b}$$

$$\tilde{Z}_{yz}(\alpha,\beta) = -\tilde{Y}_{yz}(\alpha,\beta)/\Delta \tag{9c}$$

$$\tilde{Z}_{yy}(\alpha,\beta) = \tilde{Y}_{zz}(\alpha,\beta)/\Delta \tag{9d}$$

$$\Delta = \tilde{Y}_{yy}\tilde{Y}_{zz} - \tilde{Y}_{yz}\tilde{Y}_{zy} \tag{9e}$$

with the admittance function terms explicitly defined as

$$\tilde{Y}_{yy}(\alpha,\beta) = p_8 \cot(\gamma_2 h_2) + p_4 \tan(\gamma_1^a h_1)/p_{11} - p_3 \tan(\gamma_1^b h_1)/p_{11} \tag{10a}$$

$$\tilde{Y}_{zy}(\alpha,\beta) = +p_7 \cot(\gamma_2 h_2) - p_2 \tan(\gamma_1^a h_1)/p_{10} + p_1 \tan(\gamma_1^b h_1)/p_{10} \tag{10b}$$

$$\tilde{Y}_{yz}(\alpha,\beta) = +p_7 \cot(\gamma_2 h_2) - p_4 p_5 \tan(\gamma_1^a h_1)/p_{11} + p_3 p_6 \tan(\gamma_1^b h_1)/p_{11} \tag{10c}$$

$$\tilde{Y}_{zz}(\alpha,\beta) = p_9 \cot(\gamma_2 h_2) + p_2 p_5 \tan(\gamma_1^a h_1)/p_{10} - p_1 p_6 \tan(\gamma_1^b h_1)/p_{10} \tag{10d}$$

$$p_7 = \alpha\beta/\gamma_2 \tag{10e}$$

$$p_8 = (k_0^2 - \beta^2)/\gamma_2 \tag{10f}$$

$$p_9 = (k_0^2 - \alpha^2)/\gamma_2 \tag{10g}$$

$$p_{10} = (p_6 - p_5)/\mu_{yy} \tag{10h}$$

$$p_{11} = (p_6 - p_5)/\mu_{zz}. \tag{10i}$$

Even though the above equations are the Green's function for the even case, they can still be used to obtain the corresponding expressions for the odd modes by applying the concept of duality.

Matrix equation (8) can now be implemented to compute the propagation constant β by applying the method described in [9]–[11]. The current density components $\tilde{J}_y$ and $\tilde{J}_z$ on the strips can also be expanded in terms of known basis functions having an appropriate behavior near the edge. Next, by applying Galerkin's technique in the Fourier domain along with Parseval's theorem, a set of algebraic equations can be obtained. Finally, by setting the determinant of the characteristic matrix equal to zero and searching for the root of the resulting equation, the propagation constant β can be found.

III. Results

To verify our calculations, the effective dielectric constant, ϵ_{eff}, of a broadside coupled microstrip line printed on the isotropic substrate is computed. The physical dimensions of the housing, b and h_2, are fixed at 4.318 mm and 5.207 mm, respectively. The striplines are on a 10-mil-thick Duroid substrate with $\epsilon_r = 2.22$ mounted in the center of the broad waveguide wall. Numerical results, which are presented in Fig. 2, are calculated at 10.0 GHz and 50.0 GHz when the ratio w/b is varying from 0.1 to 0.5. The upper curves are for the odd mode, whereas the lower two are for the even mode. The results show that for the even mode, ϵ_{eff} decreases with frequency; however, for the odd mode, the opposite is true. Displayed in Fig. 2 are also data reproduced from [3], and a comparison shows excellent agreement for both even and odd modes throughout the entire computed range.

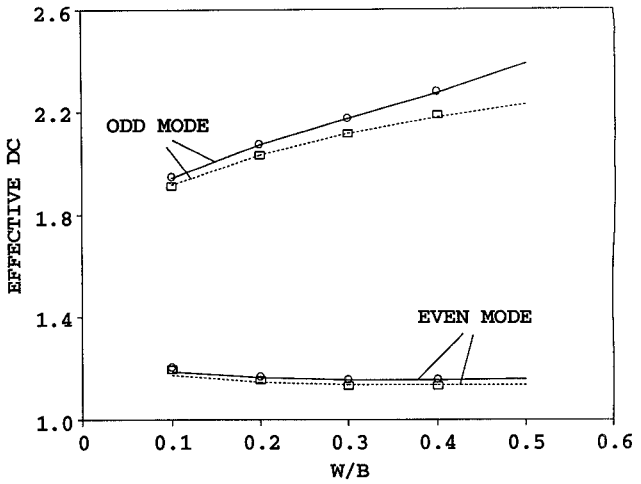

Fig. 2. Effective dielectric constant versus the ratio w/b with $b = 4.318$ mm, $h_1 = 0.127$ mm, $h_2 = 5.207$ mm, $\epsilon_{xx} = \epsilon_{yy} = \epsilon_{zz} = 2.22$, and $\mu_{xx} = \mu_{yy} = \mu_{zz} = 1.0$ ——— Data computed by this method at 10.0 GHz. ------- Data computed by this method at 50.0 GHz. ○○○ □□□ Mizuno *et al.* [3].

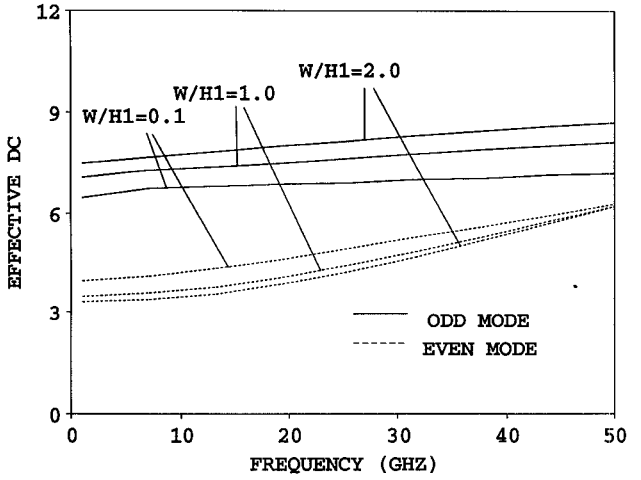

Fig. 3. Effective dielectric constant versus frequency of lines on Epsilam-10 with $b = 4.318$ mm, $h_1 = 0.254$ mm, $h_2 = 5.08$ mm, $\epsilon_{xx} = 10.3$, $\epsilon_{yy} = \epsilon_{zz} = 13.0$, and $\mu_{xx} = \mu_{yy} = \mu_{zz} = 1.0$.

To study the anisotropy effect on ϵ_{eff} and on the propagation β, the broadside coupled structure is selected to have different uniaxial substrates, with its physical dimensions being slightly different from those in the previous case. A family of curves is generated from 1.0 GHz to 50.0 GHz with respect to different w/h_1 ratios. Fig. 3 shows the response of ϵ_{eff} with the quantity w/h_1 varying from 0.1 to 2.0 for an Epsilam-10 substrate with $\epsilon_{xx} = 10.3$ and $\epsilon_{yy} = \epsilon_{zz} = 13.0$. Evidently, as the ratio w/h_1 increases, the ϵ_{eff} of the even mode also increases, which is in contrast to the smooth behavior of ϵ_{eff} for the odd mode. Notice also that, for the even mode, all curves seem to merge in the vicinity of 50.0 GHz. This behavior suggests that the β's for these selected sizes of the structure approach the equiphase point.

The data shown in Fig. 4 and Fig. 5 are for boron nitride and sapphire substrates, respectively. For boron nitride, the medium parameters are $\epsilon_{xx} = 3.4$ and $\epsilon_{yy} = \epsilon_{zz} = 5.12$, and the computed ϵ_{eff} for both modes appears to remain relatively constant for most parts of the computed frequency range. However, for

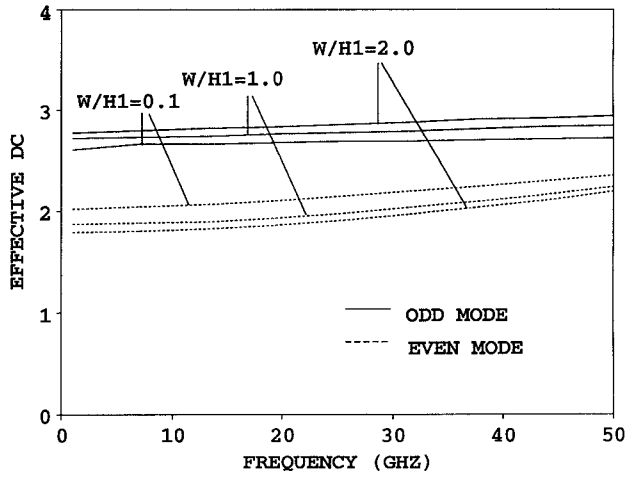

Fig. 4. Effective dielectric constant versus frequency of lines on boron nitride with $b = 4.318$ mm, $h_1 = 0.254$ mm, $h_2 = 5.08$ mm, $\epsilon_{xx} = 3.4$, $\epsilon_{yy} = \epsilon_{zz} = 5.12$, and $\mu_{xx} = \mu_{yy} = \mu_{zz} = 1.0$.

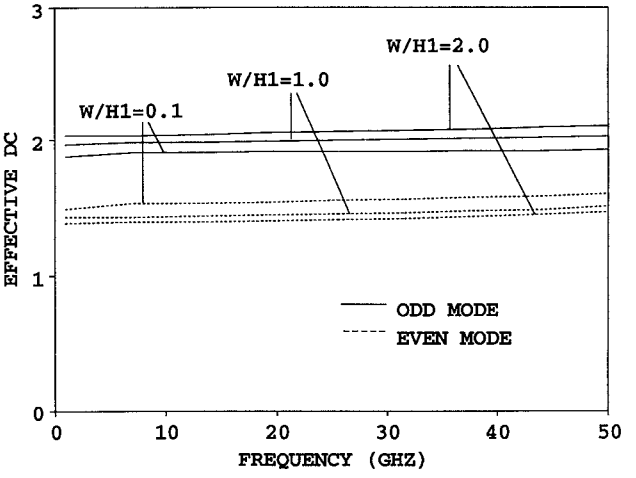

Fig. 6. Effective dielectric constant versus frequency of lines on PTFE cloth with $b = 4.318$ mm, $h_1 = 0.254$ mm, $h_2 = 5.08$ mm, $\epsilon_{xx} = 2.45$, $\epsilon_{yy} = 2.89$, $\epsilon_{zz} = 2.95$, and $\mu_{xx} = \mu_{yy} = \mu_{zz} = 1.0$.

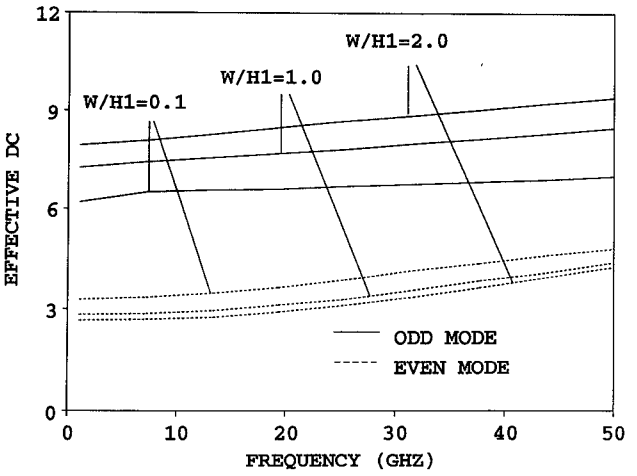

Fig. 5. Effective dielectric constant versus frequency of lines on sapphire with $b = 4.318$ mm, $h_1 = 0.254$ mm, $h_2 = 5.08$ mm, $\epsilon_{xx} = 11.6$, $\epsilon_{yy} = \epsilon_{zz} = 9.4$, and $\mu_{xx} = \mu_{yy} = \mu_{zz} = 1.0$.

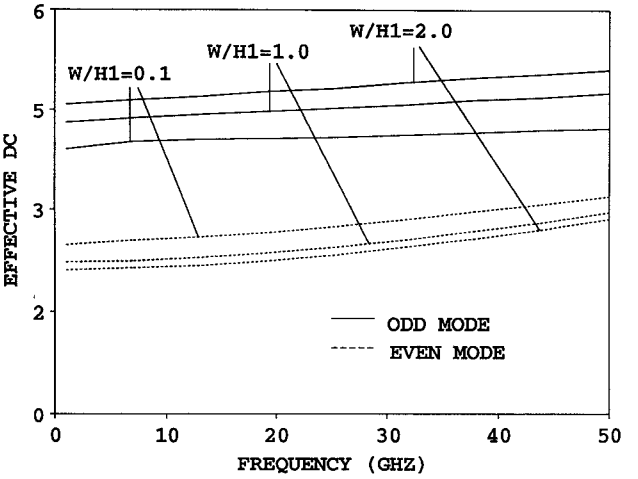

Fig. 7. Effective dielectric constant versus frequency of lines on glass cloth with $b = 4.318$ mm, $h_1 = 0.254$ mm, $h_2 = 5.08$ mm, $\epsilon_{xx} = 6.24$, $\epsilon_{yy} = 6.64$, $\epsilon_{zz} = 5.56$, and $\mu_{xx} = \mu_{yy} = \mu_{zz} = 1.0$.

the sapphire, which is characterized by $\epsilon_{xx} = 11.6$ and $\epsilon_{yy} = \epsilon_{zz} = 9.4$, the ϵ_{eff} of the odd mode is much more sensitive to changes in the w/h_1 ratio than for the even mode.

The study of anisotropic effects on the propagation characteristics of shielded broadside coupled lines using biaxial substrates is also carried out. All dimensions are taken to be the same as before, but the parameters that were allowed to change were the elements of the permittivity tensor $[\epsilon]$. Figs. 6 and 7 show how the effective dielectric constant changes when the filled PTFE (glass cloth) and the plain PTFE cloth are used as the material substrates. The tensor elements of permittivity $\epsilon_{xx} = 2.45$, $\epsilon_{yy} = 2.89$, and $\epsilon_{zz} = 2.95$ were used in the computations performed for the PTFE cloth. Since the tensor values of ϵ_{yy} and ϵ_{zz} differ only by a small amount, the calculated data for this case are almost the same when compared with the substrate, which is treated as a uniaxial material. The expanded scale shows that the change is almost linear over the frequency range from 1.0 GHz to 50.0 GHz. However, in the latter case, when the material parameters of the glass cloth $\epsilon_{xx} = 6.24$, $\epsilon_{yy} = 6.64$, and $\epsilon_{zz} = 5.56$ are used for computations, they show a greater variation in ϵ_{eff} than that observed earlier for the PTFE cloth. In addition to the two above cases, numerical results for lithium niobate with $\epsilon_{xx} = 43.0$ and $\epsilon_{yy} = \epsilon_{zz} = 28.0$ are also shown in Fig. 8. In this case, the response of β with frequency for both the odd and even modes as the ratio w/h_1 changes from 0.1 to 1.0 is displayed, from which it is quite clear that higher values of the permittivity result in a substantial variation of the propagation constant.

Finally, to illustrate the versatility of the developed formulation and its spectral-domain implementation, the substrates of the broadside coupled line are chosen to be biaxially anisotropic in both of $[\epsilon]$ and $[\mu]$. Here, Fig. 9 shows how the magnetic anisotropy effect would change the propagation constant β as values of the permeability $[\mu]$ tensor increase from 2.75, 2.25, and 5.0 to 3.75, 3.25, and 6.00 in increments of 0.5, written respectively for μ_{xx}, μ_{yy}, and μ_{zz}. It is interesting to see that for the even mode, the propagation constant is almost insensitive to the variation of tensor permeability $[\mu]$ until the frequency passes the 25.0 GHz point, whereas for the odd mode β displays a sensitivity to changes in elements of $[\mu]$ around

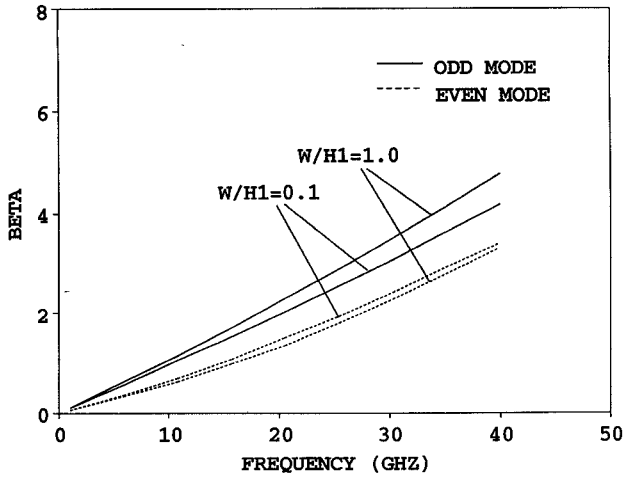

Fig. 8. Propagation constant versus frequency of lines on lithium niobate with $b = 4.318$ mm, $h_1 = 0.254$ mm, $h_2 = 5.08$ mm, $\epsilon_{xx} = 43.0$, $\epsilon_{yy} = \epsilon_{zz} = 28.0$, and $\mu_{xx} = \mu_{yy} = \mu_{zz} = 1.0$.

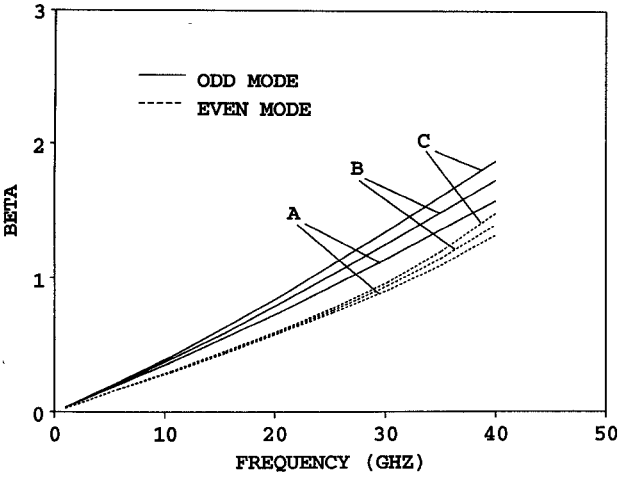

Fig. 9. Propagation constant versus frequency of lines on substrate characterized by $\epsilon_{xx} = 2.0$, $\epsilon_{yy} = 2.35$, and $\epsilon_{zz} = 3.50$ with $b = 4.318$ mm, $h_1 = 0.50$ mm, $h_2 = 4.834$ mm, and $w = 0.5$ mm. A: $\mu_{xx} = 2.75$, $\mu_{yy} = 2.25$, $\mu_{zz} = 5.00$. B: $\mu_{xx} = 3.25$, $\mu_{yy} = 2.75$, $\mu_{zz} = 5.50$. C: $\mu_{xx} = 3.75$, $\mu_{yy} = 3.25$, $\mu_{zz} = 6.00$.

10.0 GHz. The results of this study indicate that anisotropy, whether electric or magnetic, is important and cannot be neglected, especially at higher frequencies.

IV. Conclusion

A rigorous analysis through an application of the spectral-domain technique for a broadside coupled microstrip line on anisotropic substrates has been presented. The new expressions for the Green's functions for both the even and odd modes are derived via the transformed fourth-order differential equations. The numerical solution is obtained by using the Galerkin method in the Fourier domain. Numerical data for the effective dielectric constant computed by this method agree well with those previously published for the special case of isotropic substrate. Effects of anisotropy on shielded lines along the E-plane direction of the waveguide printed on different uniaxial and biaxial substrates are studied with respect to different strip widths. It is observed that generally, for all treated cases, the odd-mode effective dielectric constant is much more sensitive to changes in the strip width than that for the even mode, especially when higher values are selected for the elements of the $[\epsilon]$ tensor. Finally, dispersion curves for both magnetically and dielectrically anisotropic substrates are also generated to illustrate their effects on the propagation constant of the broadside coupled line.

References

[1] J. L. Allen and M. F. Estes, "Broadside coupled strips in a layered dielectric medium," *IEEE Trans. Microwave Theory Tech.*, vol. MTT-20, pp. 662–669, Oct. 1972.

[2] J. Bornemann, "Anwendung der methode der orthogonalreihenentwicklung auf quasiplanaare structuren mit homogenem und inhomogenem dielecktrikum," Ph.D. thesis, Univ. of Bremen, West Germany, 1984.

[3] H. Mizuno, C. J. Verver, R. J. Douville, and M. G. Stubbs, "Propagation in broadside coupled suspended-substrate stripline in E-plane," *IEEE Trans. Microwave Theory Tech.*, vol. MTT-33, pp. 946–951, Oct. 1985.

[4] N. G. Alexopoulos, "Integrated Circuit structures on anisotropic substrates," *IEEE Trans. Microwave Theory Tech.*, vol. MTT-33, pp. 847–881, Oct. 1985.

[5] A. G. D'Assunçao, A. J. Giarola, and D. A. Rogers, "Characteristics of broadside coupled microstrip lines with iso/anisotropic substrates," *Electron. Lett.*, vol. 17, no. 7, pp. 264–265, Apr. 1981.

[6] S. K. Koul and B. Bhat, "Transverse transmission line method for the analysis of broadside coupled microstrip lines with anisotropic substrates," *Arch. Elek. Übertragung.*, vol. 37, pp. 59–64, Jan./Feb. 1983.

[7] T. Q. Ho and B. Beker, "Spectral-domain analysis of shielded microstrip lines on biaxially anisotropic substrates," pp. 1017–1021, this issue.

[8] L. P. Schmidt and T. Itoh, "Spectral domain analysis of dominant and higher order modes in finline," *IEEE Trans. Microwave Theory Tech.*, vol. MTT-28, pp. 981–985, Sept. 1980.

[9] T. Itoh and R. Mittra, "Spectral domain approach for calculating the dispersion characteristics of microstrip lines," *IEEE Trans. Microwave Theory Tech.*, vol. MTT-21, pp. 496–499, July 1973.

[10] T. Itoh, "Analysis of microstrip resonators," *IEEE Trans. Microwave Theory Tech.*, vol. MTT-22, pp. 946–952, Nov. 1974.

[11] Y. C. Shih and T. Itoh, "Analysis of transmission lines on semiconductor substrate," Univ. of Texas Microwave Laboratory Rep. No. 84-2, Mar. 1984.

Picosecond Pulse Propagation in Coplanar Waveguide Forward Directional Couplers

P. Singkornrat and J. A. Buck

Abstract—**The spectral-domain method is used to calculate the frequency-dependent even- and odd-mode effective dielectric constants of symmetric coplanar waveguide forward directional couplers. Comparisons are made with symmetric microstrip forward couplers on the same substrate that have the same line spacing and access port characteristic impedance. Results indicate that certain coplanar designs will have lower loss and greater bandwidth than the microstrip devices. Picosecond pulse propagation in both structures is studied using the calculated dispersion data.**

Manuscript received May 3, 1990; revised January 22, 1991. This work was supported by IBM Boca Raton through the IBM Resident Study Program.

The authors are with the School of Electrical Engineering, Georgia Institute of Technology, Atlanta, GA 30332.

IEEE Log Number 9144280.